A Strategy for the Revival of Electric Machines and Drives Courses

Ned Mohan Mahmoud Riaz Paul Imbertson Ted Brekken

Department of Electrical and Computer Engineering
University of Minnesota
Minneapolis, MN 55455 USA
Email: mohan@ece.umn.edu

Abstract

All over the world, the courses in electric machines and electric drives are suffering from lack of student interest, leading to their cancellation and eventual elimination from the curriculum. This is happening just when we need trained students to make use of tremendous opportunities in this field. This article presents a proven strategy that has more than doubled (almost tripled) the student enrollment from its low point at the University of Minnesota. This approach, presented at three NSF-sponsored Faculty Workshops held at the University of Minnesota [1], is now backed up by a recently-published textbook [2]. The development underway of a DSP-based laboratory [3] has the potential of making the first course on this topic one of the the most sought-after in the EE curriculum, attracting a large number of students from other disciplines such as mechanical, civil and environmental engineering.

OPPORTUNITIES

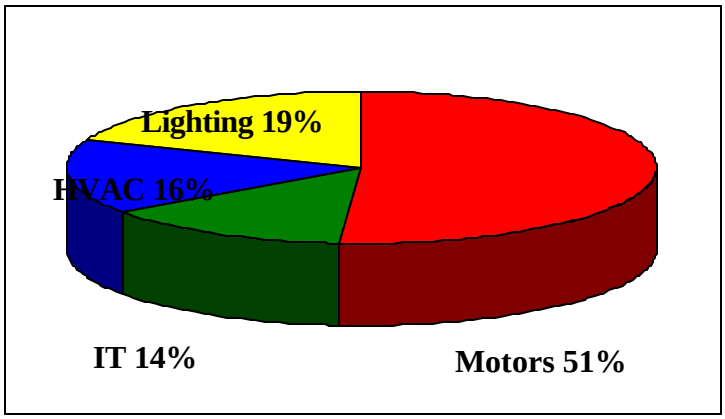

Fig. 1 World's electricity consumption.

The pie chart of Fig. 1 shows that motors consume over one-half of the electricity generated in the world. Using these motors more efficiently would obviate the need for more power plants and the energy conserved would be green – money saved and less damage to the environment. By some accounts, proven technologies in this field if applied in the United States in the industrial systems alone can save the electricity annually used by the entire state of New York [4]! There are exciting new applications: hybrid-electric vehicles promise to increase the gas mileage to over 60 miles per gallon, windmills requiring electric drives to feed power into the constant-frequency grid promise to make a substantial contribution to the energy supply of the future. Factory automation and robotics are needed for improved industrial productivity in face of global competition. Not only are these applications of immense environmental and societal importance, they also catch the imagination of young students.

Electric Machines versus Electric Drives

The introductory course in electric machines has not changed in decades – no wonder students look upon the subject of electric machines as old-fashioned, staid and boring. But the solution couldn't be simpler – in the same course we can shift the focus from electric machines to electric drives (Fig. 2), which allow us to introduce this subject in the context of exciting new applications. Even a mundane application of driving

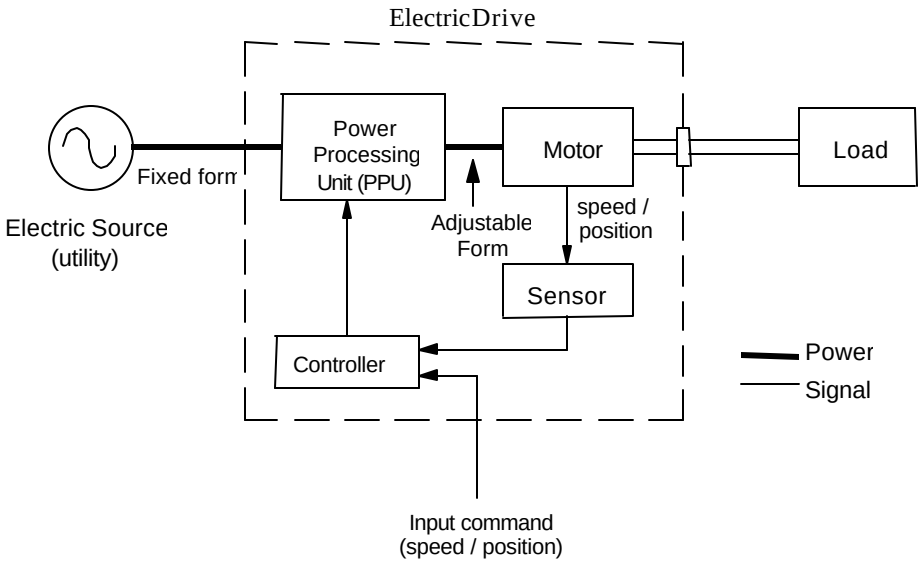

Fig. 2 Block diagram of an electric drive system.

compressors within air-conditioners becomes exciting if adjustable-speed-driven compressors by capacity modulation can be shown to consume 30% less energy compared to their conventional counterparts with on/off cycling to maintain temperature [5].

Meeting the Challenge - Developing A New Approach

Without the prerequisite of electric machine theory, how can we discuss the subsystems that make up electric drives (Fig. 2) in a single-semester course? Such a course, consistent with the university mission, must stress the fundamentals thus providing continuity to advanced graduate-level courses in this field, while preparing students for industrial assignments. This challenge has several components that are discussed below.

Deleting Irrelevant Topics. The above challenge required a completely fresh look at what topics are covered and how they are covered in the traditional course in this field. To begin with, many of the topics such as using brush-type dc machines as generators and their various field-winding connections were omitted. Discussing outmoded applications wastes valuable course time and worse yet, it gives students the wrong impression that these practices may still be relevant.

Discussion of the Power Processing Unit. In electric drives (Fig. 2), power electronic converters play an important role, as a power processing unit (PPU), of efficiently converting utility-supplied power to voltages and currents of appropriate phase, frequency and amplitude, best suited for the operating conditions. These converters are discussed in the power electronics course in detail, but need to be covered in only three to four lectures in the introductory drives course. In the block diagram of the PPU for

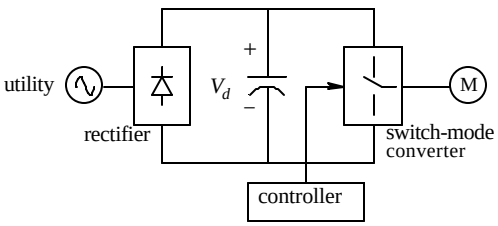

Fig. 3 Block diagram of PPUs.

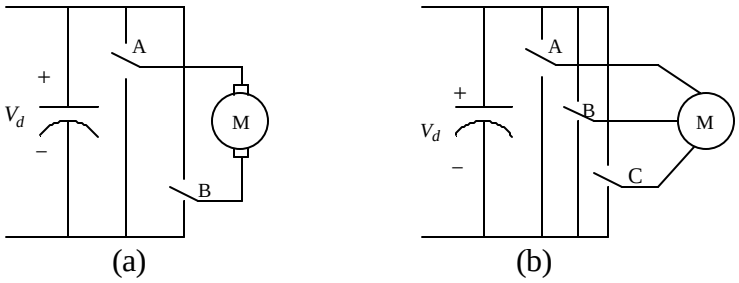

Fig. 4 Switch mode converters for (a) dc- and (b) ac-motor drives.

modern drives (Fig. 3), the utility interface and the interactions between the drive and the utility can be covered as a separate topic (time permitting) under the heading of Power Quality Issues. More important is to describe the switch-mode pulse-width-modulated (PWM) converter, which from a constant amplitude dc input voltage synthesizes the required output to the motor in phase, frequency and amplitude.

The switch-mode converters for dc-motor and ac-motor drives are shown in Fig. 4 consisting of two poles and three poles respectively. Each pole (a bi-positional switch) is treated as a building block. This building block (Fig. 5a) is a two-port, a voltage port on

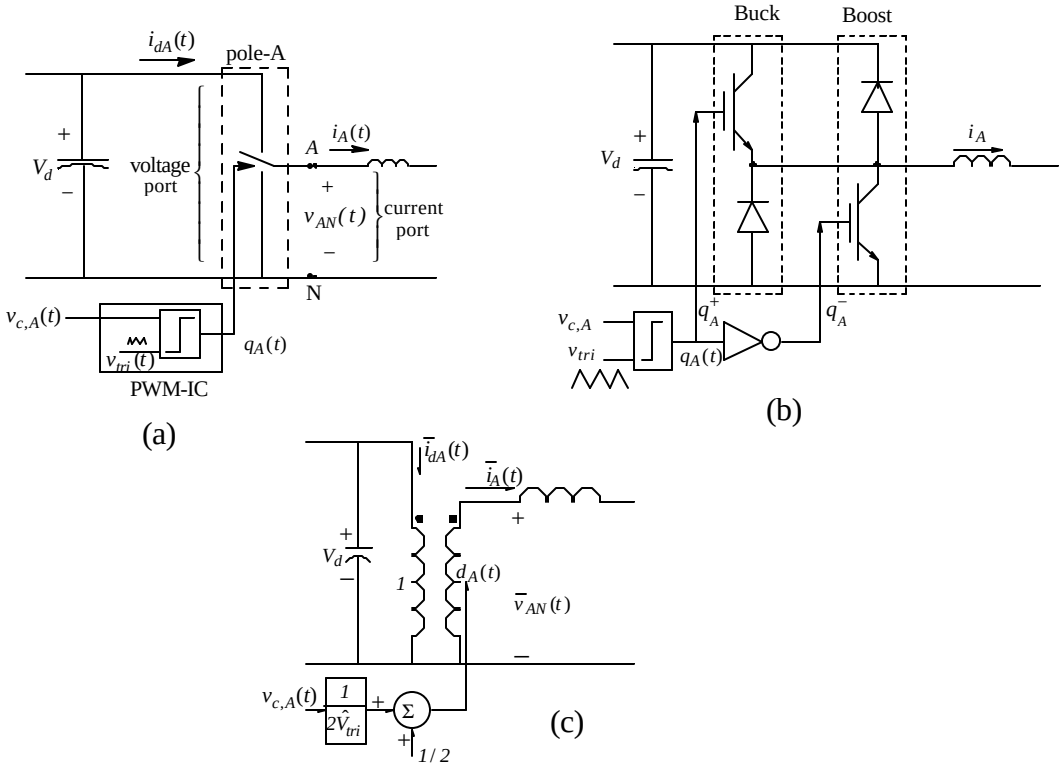

Fig. 5 Ideal transformer equivalent of a single pole.

one side and the current port on the other. The desired output is synthesized by pulse-width-modulating (PWM) the bi-positional switch at a high switching frequency (20 kHz is typical in small drives). The bi-positional switch is realized (Fig. 5b) by means of two transistors and two diodes, constituting a buck converter (for $i_A > 0$) in parallel with a boost converter (for $i_A < 0$). For a clear yet concise understanding of the pulse-width-modulation operation for synthesis purposes, we can assume the switching frequency to be infinite, thus relating the instantaneous-average quantities, if this paradoxical expression may be used, at the two ports of this bi-positional switch by an ideal transformer (Fig. 5c) with a continuously controllable turns-ratio.

Note that the time-dependent, instantaneous-average quantities are represented by lower-case letters with a "-" on top. Thus the switch-mode converter, for example for the ac-motor drives in Fig. 4b can be quickly analyzed by its representation in Fig. 6, giving

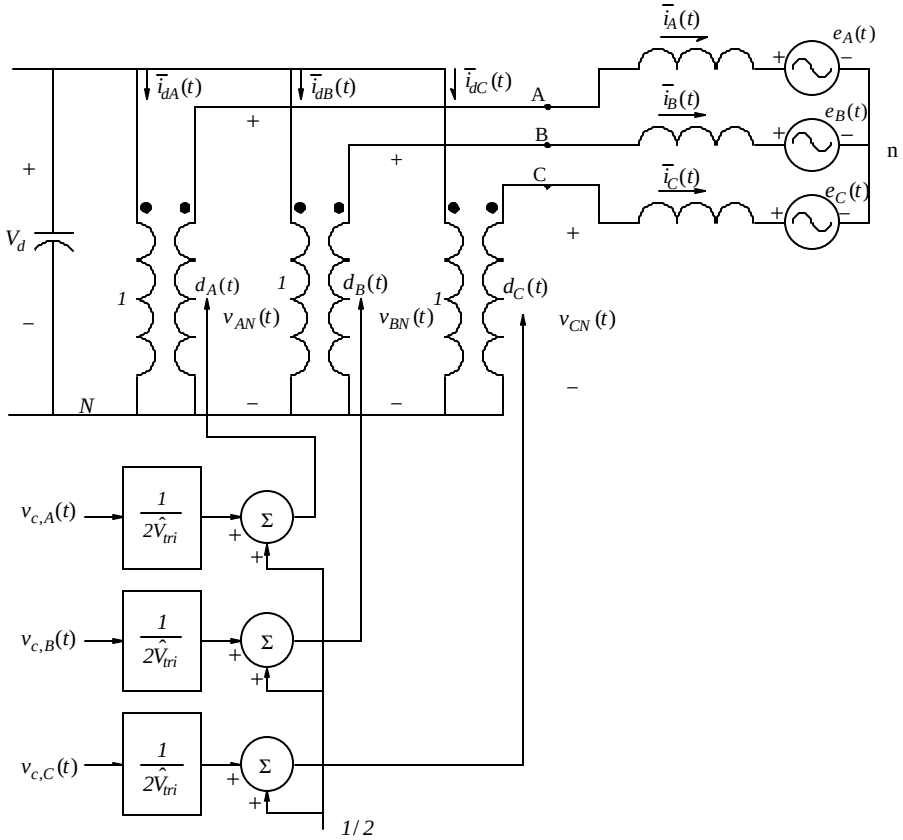

Fig. 6 Average representation of the three phase converter.

students a clear understanding of the synthesis process using PWM in switch-mode converters and the relationship between the ac-side and the dc-side quantities.

Direct Computation of Electromagnetic Torque. With the goal of discussing speed and position control by electric drives (uncontrolled machines form a subset of these), the machine analysis requires a new approach to understanding the physical basis on which ac and dc machines operate, thus allowing a clear understanding of how they ought to be controlled in electric drives for optimum performance in speed and position control applications. Therefore the electromagnetic torque, which is the fundamental control variable for controlling speed and position is computed directly from the flux density and conductor currents ($f_{em} = B\ell i$), rather than by traditional means of computing it as power divided by speed. The same is true for the computation of the induced back-emf in all machines, the mechanism by which machines absorb power from the electrical source. This procedure clearly shows the commonality between various machines, all having their torque constant k_T equal to their voltage constant k_E.

Utilizing Space-Vectors for the Analysis of AC Machines. The key development to the analysis of ac machines has been the use of space vectors in a very simple form in the first undergraduate course in this field. The following paragraphs outline how space vectors are introduced in a physical easy-to-understand basis, and how they allow the "brushless-dc" and induction machines to be analyzed (in steady state only in this introductory course, however establishing a solid foundation for their dynamic and vector-control analysis in advanced-level courses) quickly; the time saved permits discussion of topics such as power electronics converters in electric drives and their adjustable-speed operation and control in a single-semester course.

Introducing Space Vectors. An analogy can be drawn to the use of phasors in circuit analysis in ac steady state: voltages and currents varying sinusoidally with time are represented by phasors ($\bar{V}$ and $\bar{I}$), which are mathematically represented by complex numbers. In ac machines, ideally each of the phase windings shown in Fig. 7a has a conductor density that is sinusoidally-distributed with respect to the magnetic axis of that

phase. At any instant of time, each phase winding produces a sinusoidal flux-density distribution (or mmf) in the air gap, which can be represented by a space vector (of the appropriate length) along the magnetic axis of that phase (or away if the phase current at that instant is negative). These mmf space vectors are $\vec{F}_a(t)$, $\vec{F}_b(t)$, and $\vec{F}_c(t)$, as shown in Fig. 7a with an "$\rightarrow$" on top of an instantaneous quantity. Assuming that there is no magnetic saturation, the resultant mmf distribution in the air gap due to all three phases at that instant can simply be represented using vector addition by the resultant space vector shown in Fig. 7b, where the subscript "s" represents the combined stator quantities:

$$\vec{F}_s(t) = \vec{F}_a(t) + \vec{F}_b(t) + \vec{F}_c(t) \qquad (1)$$

The above explanation provides a physical basis for understanding space vectors. We should note that unlike phasors, space vectors are also applicable under dynamic conditions – thus their use also lays the foundation for advanced courses - because the sinusoidal air gap flux-density distribution is produced by the sinusoidally-distributed phase windings of each of the stator phases shown in Fig. 7a (the currents producing the mmf may even be dc or any other waveform).

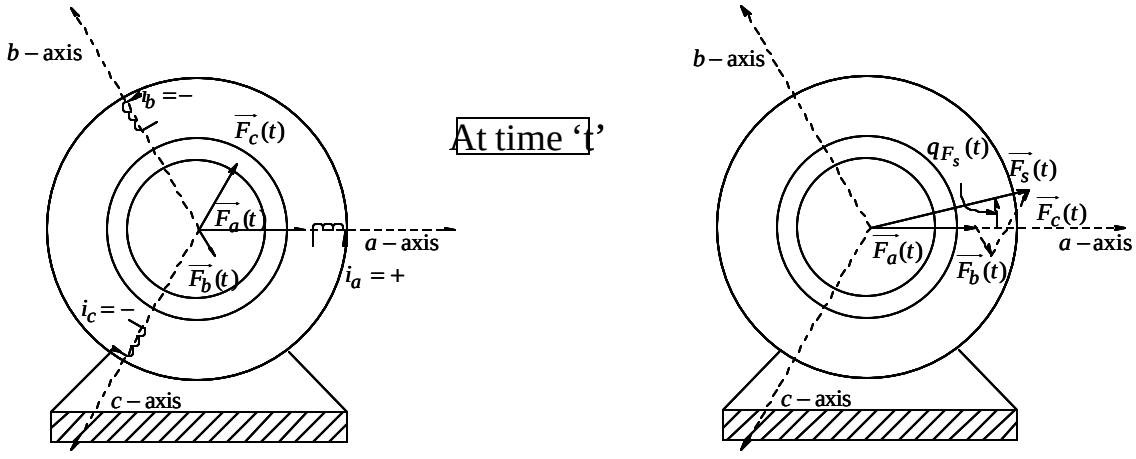

(a) (b)

Fig. 7 MMF representation by space vector

The currents and voltages of phase windings are treated as terminal quantities. Their resultant stator current and the stator voltage space vectors are calculated by multiplying instantaneous phase values by the winding orientations shown in Fig. 7a:

$$\vec{i_s}(t) = i_a(t)\angle 0^0 + i_b(t)\angle 120^0 + i_c(t)\angle 240^0 = \hat{I}_s(t)\angle q_{i_s}(t) \qquad (2)$$

and,

$$\vec{v_s}(t) = v_a(t)\angle 0^0 + v_b(t)\angle 120^0 + v_c(t)\angle 240^0 = \hat{V}_s(t)\angle q_{v_s}(t) \qquad (3)$$

The stator current space vector $\vec{i_s}(t)$ lends itself to a very useful and simple physical interpretation shown by Fig. 8:

At a time instant t, the three stator phase currents in Fig. 8a result in the same mmf acting on the air gap (hence the same flux-density distribution) as that produced by $\vec{i_s}(=\hat{I}_s\angle q_{i_s})$, that is by a current equal to its peak value $\hat{I}_s$ flowing through a hypothetical sinusoidally-distributed winding shown in Fig. 8b, with its

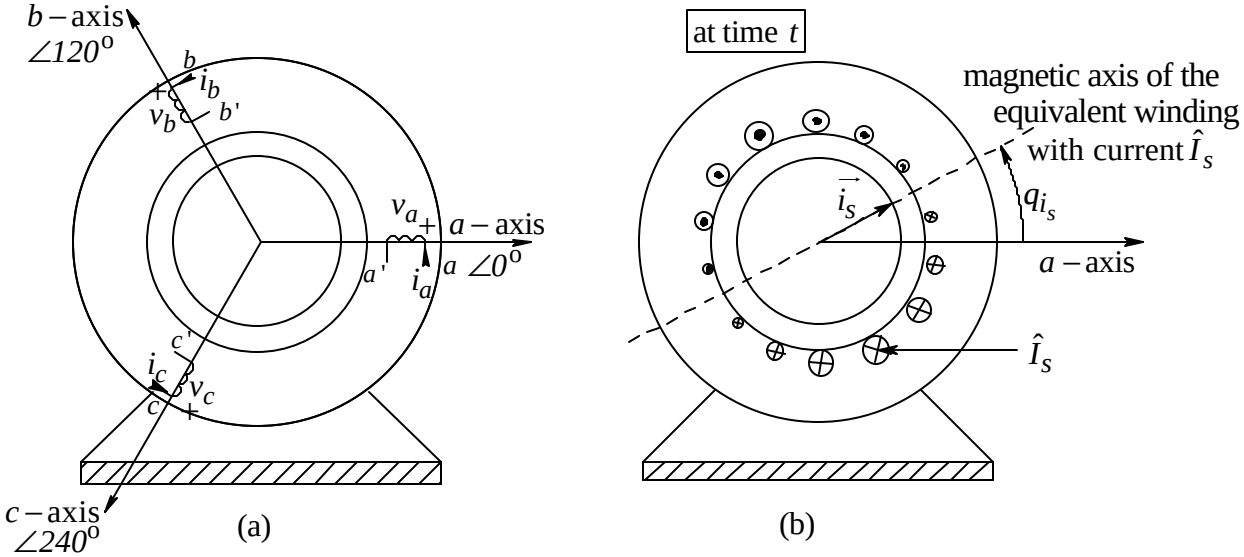

Fig. 8 (a) Phase voltages and currents; (b) physical interpretation of stator current space vector.

magnetic axis oriented at $q_{i_s}\,(=q_{F_s})$. This hypothetical winding has the same number of turns sinusoidally-distributed as any of the phase windings.

The above physical explanation not only permits the stator current space vector to be visualized, but it also simplifies the derivation of the electromagnetic torque, which can now be calculated on just this single hypothetic winding, rather than having to calculate it separately on each of the phase windings and then summing it.

Relating Phasors to Space Vectors in Sinusoidal Steady State. The introductory course only deals with the sinusoidal steady state. Under such a condition, the voltage and current phasors in phase *a* have the same orientation as the stator voltage and current space vectors at time $t=0$, as shown for the current in Fig. 9; the amplitudes are related by a factor of $2/3$. This relationship greatly simplifies the derivation of equivalent circuits in sinusoidal steady state, as discussed later on.

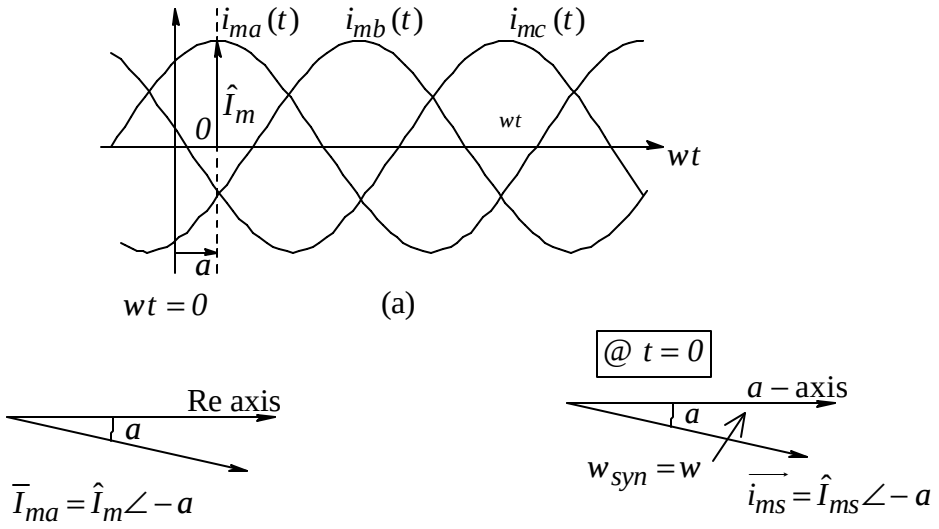

Fig. 9 Relationship between space vectors and phasors in balanced sinusoidal steady state.

Discussing "Brush-less DC" Motor Drives. Utilizing space vectors, we require only 2 to 3 lectures to discuss brushless-dc (PMAC) motor drives (Fig. 10) that are often used in high performance systems.

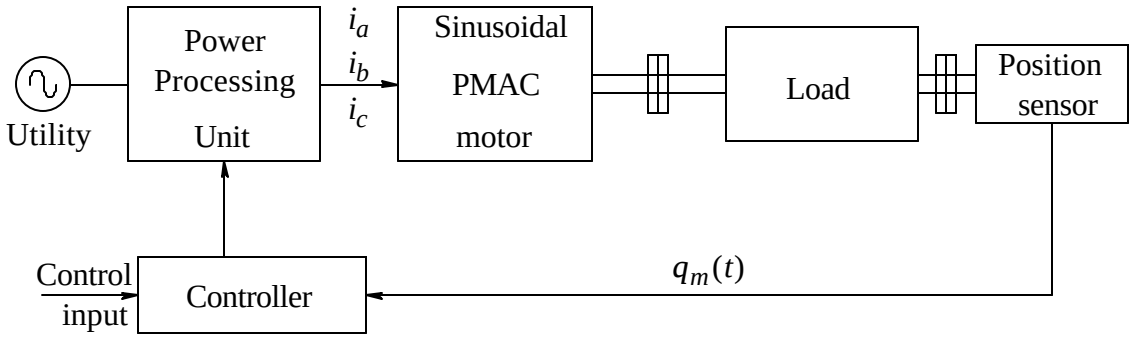

Fig. 10 Block diagram of the closed loop operation of a PMAC drive.

The permanent magnets on the rotor (Fig. 11a) produce a sinusoidal flux-density distribution that is represented by the space vector $\vec{B}_r(t)$, whose orientation depends of the rotor position q_m, which is measured. The stator phase currents are controlled such as to place the stator current space vector $\vec{i}_s(t)$ 90^0 ahead of $\vec{B}_r(t)$ in the direction of rotation, as shown in Fig. 11b.

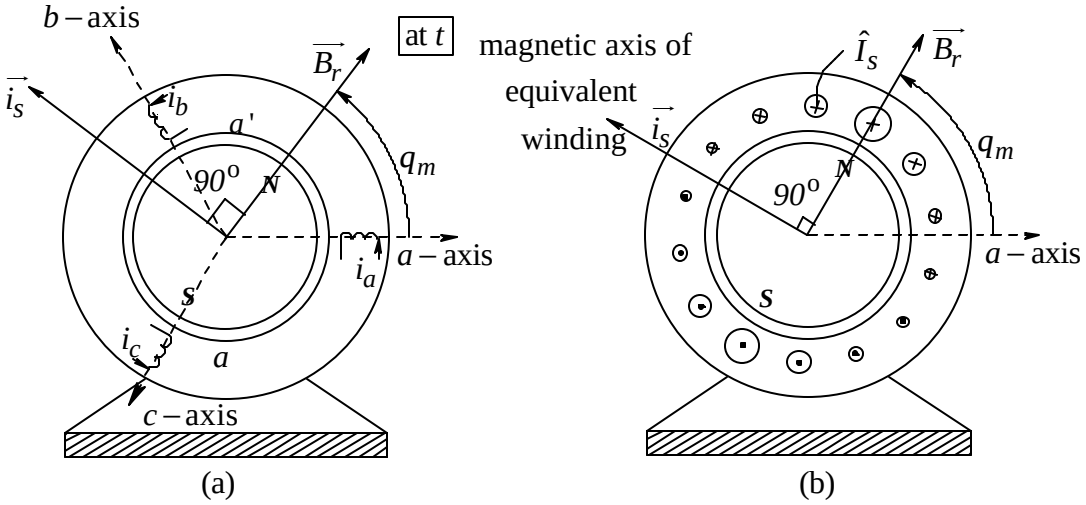

Fig. 11 Stator current space vector and rotor field space vector in a PMAC drive.

We can easily compute the electromagnetic torque on the stator (the rotor toque will be equal and opposite) in a physical basis in Fig. 12. At any instant, the stator-current produced mmf can be represented by a hypothetical sinusoidally-distributed winding with its magnetic axis along $\vec{i}_s(t)$. We can simplify the computation by assuming $q_m = 0$ in Fig. 12. Using the basic equation ($f_{em} = B\ell i$), the torque on the conductors (in this equivalent sinusoidally-distributed winding with N_s turns, all conductors carry a current $\hat{I}_s$) in a magnetic field in a differential angle dx can be expressed as follows:

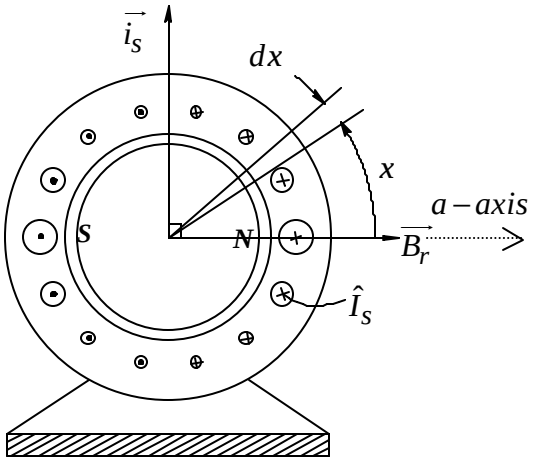

Fig. 12 Torque calculation on the stator.

$$dT_{em}(x) = r \underbrace{\hat{B}_r \cos x}_{flux\,density\,at\,x} \cdot \underbrace{\ell}_{cond.length} \cdot \hat{I}_s \cdot \underbrace{\frac{N_s}{2} \cos x \cdot dx}_{diff\ no\ of\ cond\ at\ x} \qquad (4)$$

Hence, integrating over all conductors and making use of symmetry

$$T_{em} = 2 \times \int_{x=-p/2}^{x=p/2} dT_{em}(x) = \left[p \frac{N_s}{2} r \ell \hat{B}_r \right] \hat{I}_s = k_T \hat{I}_s \qquad (5a)$$

where, k_T is the machine torque constant

$$k_T = p\frac{N_s}{2} r\,\ell\,\hat{B}_r \qquad (5b)$$

Eq. 5 clearly shows that the torque developed depends linearly on $\hat{I}_s$ (if $\hat{B}_r$ is constant); a similarity to brush-type dc machines that has led to the name "brushless dc" drives in the trade literature.

Using space vectors, we can quickly show that due to the rotating field distribution represented by $\vec{B}_r(t)$, a back-emf is induced in each of the stator phase windings, which in steady state is in phase with the phase current (Fig. 13), and whose amplitude is given by

$$\hat{E}_f = k_E w_m \qquad \text{where} \qquad k_E = k_T, \qquad (6)$$

once again underscoring the similarity to the brush-type dc machines. The rotating mmf produced by the three stator phase currents also induces an emf in the stator phase windings; this emf can be represented by a voltage drop across the magnetizing inductance and the leakage inductance $L_s(=L_m+L_{\ell s})$ in Fig. 13. The effect of the stator winding resistance R_s can be included to complete the per-phase equivalent circuit.

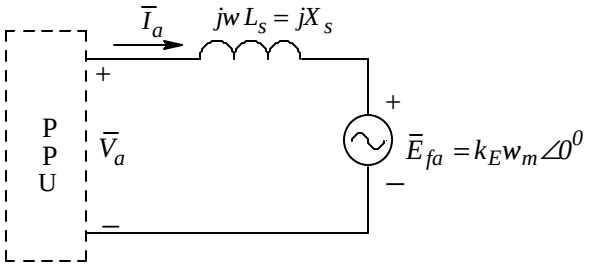

Fig. 13 Per-phase equivalent circuit.

A simple hysteretic controller using a current-regulated PWM inverter can be described (Fig. 14) pointing out that a space-voltage-vector-modulated inverter will be covered in the advanced course [6] to keep switching frequency constant.

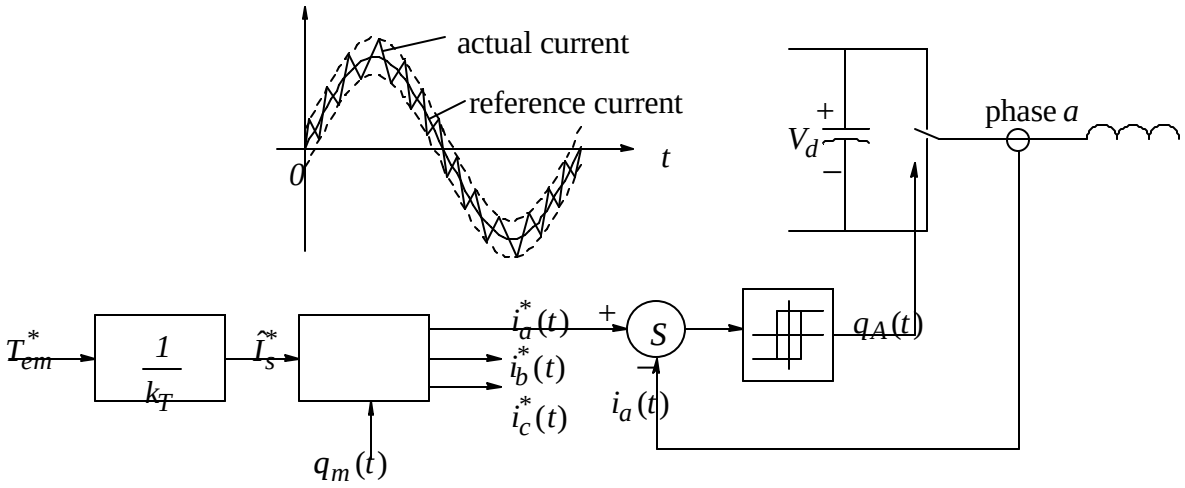

Fig. 14 Hysteretic Controller for PMAC Drives.

Discussing Induction- Motor Drives.

Use of space vectors allows induction machines to be analyzed very easily, at the same time establishing the foundation for speed and vector control. The steady state analysis does not require the squirrel-cage to be represented by three-phase wound rotor and a clear picture is presented how the electromagnetic torque depends on 1) the amplitude and 2) the relative (slip) speed of the rotating flux-density distribution "cutting" the rotor bars. It is of immense benefit to initially neglect the stator winding resistances and leakage inductances (introduced later) – this assumption defines the air gap flux density in the air gap as the time-integral of the applied voltages; nothing in the rotor circuit can change that.

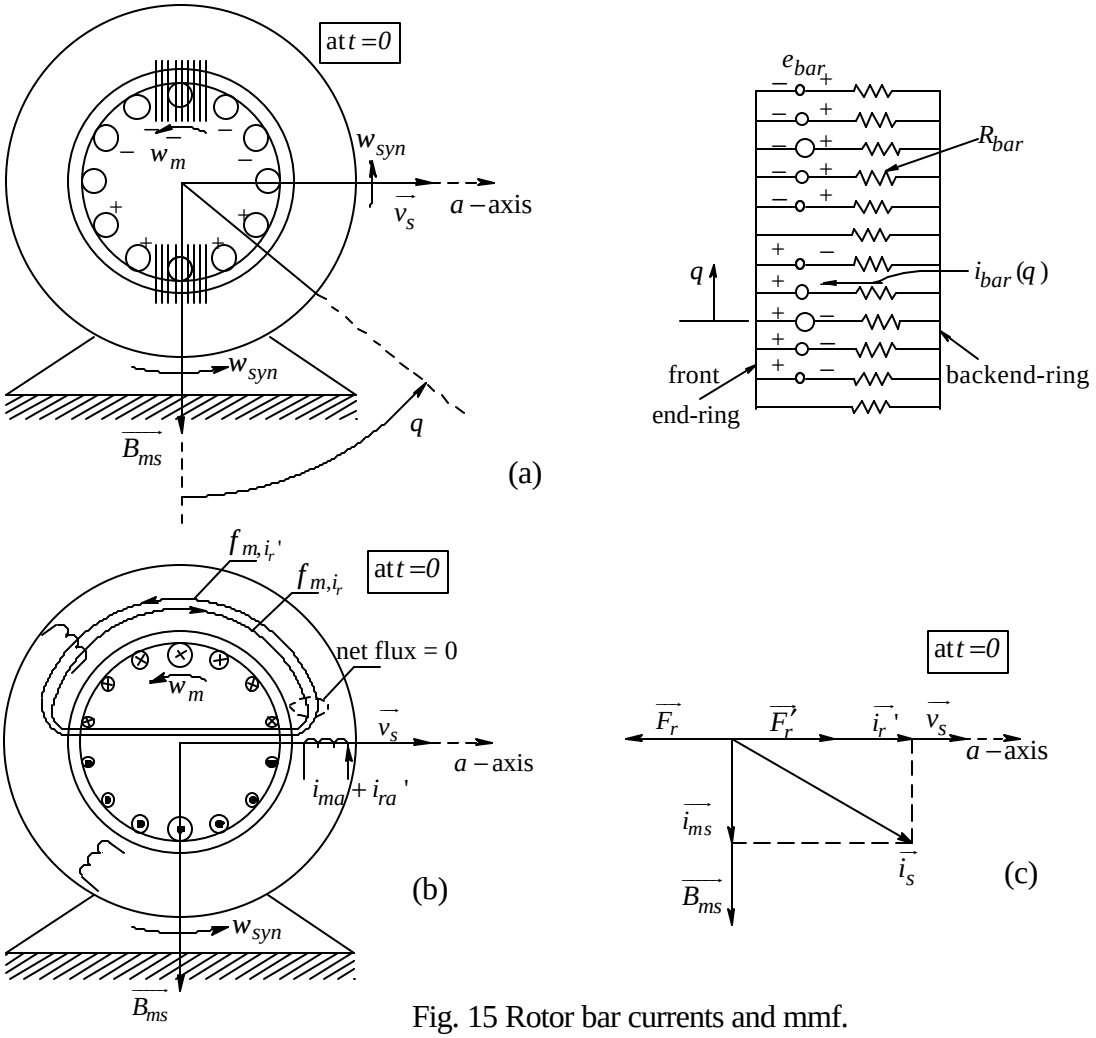

Fig. 15 Rotor bar currents and mmf.

We can show that the flux-density distribution rotating at the synchronous speed w_{syn} (at a slip speed w_{slip} relative to the rotor speed w_m) induces voltages in the rotor bars. Further assuming the rotor leakage flux (included later) to be zero, the currents in the short-circuited rotor bars have the current distribution shown in Fig. 15a and b – bars "cutting" the maximum flux-density have the highest induced voltages and hence highest currents represented by the biggest circles. The sinusoidally-distributed mmf distribution due to the rotor cage allows it to be represented by a space vector $\vec{F}_r$ (Fig. 15c). In response to $\vec{F}_r$, the stator windings draw additional currents, represented by the space vector $\vec{i}_r'$, to nullify $\vec{F}_r$, thus keeping the air gap flux density unchanged (it cannot

change because we have assumed the stator winding resistances and leakage inductances to be zero).

At a later time t_1 (Fig. 16), the distribution has rotated in the air gap but their relative positions remain the same. This shows that the rotor-produced mmf is always lagging the flux-density space vector by 90^0, hence also rotating at the synchronous speed, independent of the rotor speed.

The electromagnetic torque can be computed (Fig. 17a) by representing the stator-produced nullifying mmf by a single sinusoidally-distributed hypothetical winding shown with a current $\hat{I}_r'$ flowing through it. The torque calculations are exactly the same as in the brushless dc-machine (Eqs. 4 and 5), and show that the torque is proportional to the peak flux density and the rotor bar currents (which in turn depend on the peak flux density and the slip speed)

$$T_{em} = k_t \hat{B}_{ms} \hat{I}_r' \qquad (7a)$$

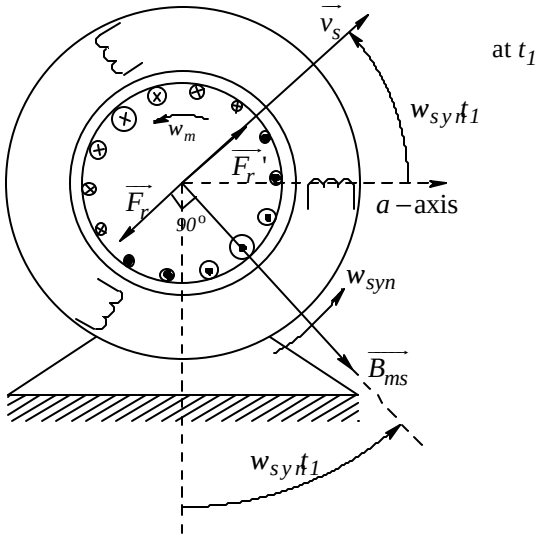

Fig. 16 Rotor produced mmf and the compensating mmf at time $t = t_1$.

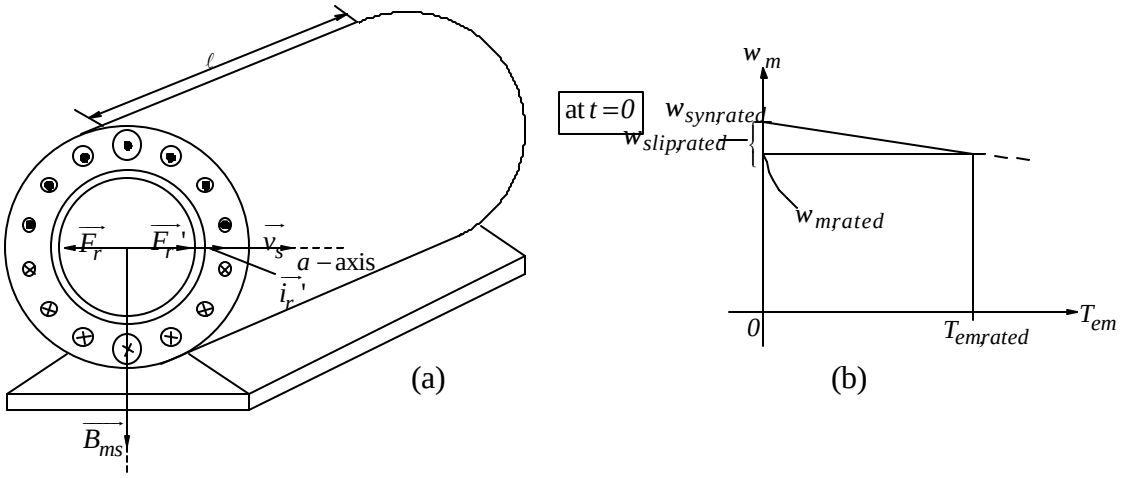

Fig. 17 Torque in induction machines.

and,

$$T_{em} = \underbrace{k_{tw}\hat{B}_{ms}^2}_{\text{constant}} w_{slip} = k_w w_{slip} \qquad (7b)$$

as shown by the torque speed characteristic in Fig. 17b.

Another important observation is that the induction machine is nearly an ideal torque producer – the stator-established air gap flux density and the rotor mmf are at the ideal angle of 90^0 (assuming the rotor-leakage flux to be zero), just like in brush-type and brushless dc machines. This type of analysis, unlike the traditional analysis that is based on the per-phase equivalent circuit, clearly indicates how the torque is produced and how it must be controlled for optimum performance. For example in adjustable speed drives with the rated speed, Eq. 7a shows that the flux-density should be kept at its maximum (that is, at the rated value) in order to minimize the I^2R losses in the rotor bars. Eq. 7b shows that keeping the air gap flux density constant at its rated value, the torque developed by the machine depends only on the slip speed as shown in Fig. 18, resulting in a family of parallel torque-speed characteristics for speed control, for various synchronous speeds corresponding to various applied frequencies.

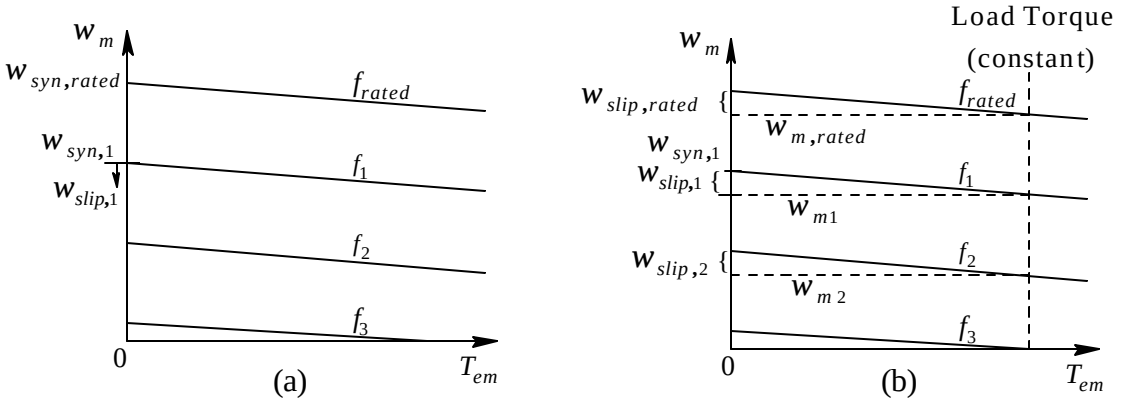

Fig. 18 Operating characteristics with a constant $\hat{B}_{ms} = \hat{B}_{ms,rated}$

This type of analysis clearly shows the generator (the regenerative braking) mode of operation at $w_m > w_{syn}$, where the rotor-bar currents (Fig. 19b) are of the opposite direction compared to that in the motoring mode (Fig. 19a with $w_m < w_{syn}$), hence the electromagnetic torque in the regenerative-braking mode acts in the direction to oppose rotation. Most wind-electric systems use electric drives with induction generators to feed power into the utility grid.

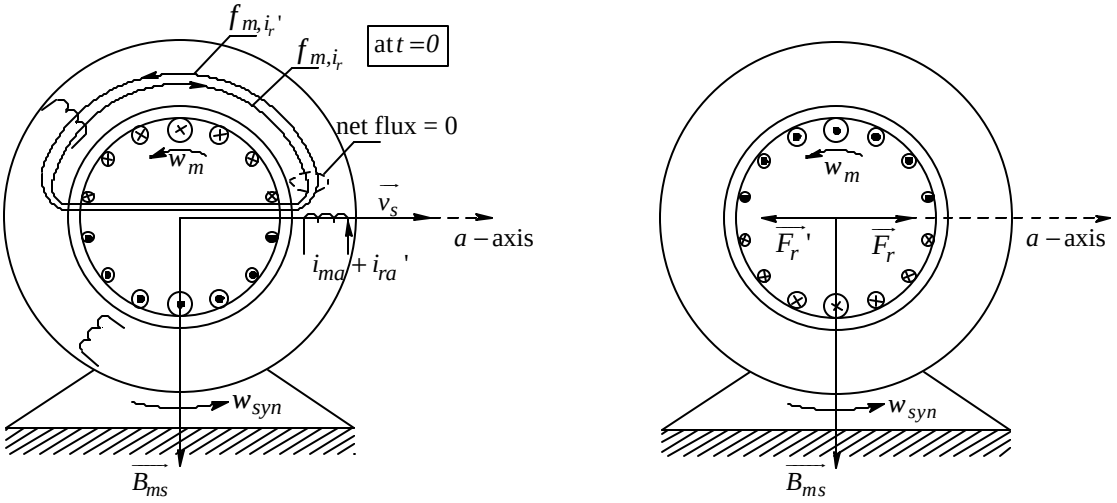

(*a*) $w_m < w_{syn}$ (*b*) $w_m > w_{syn}$

Fig. 19 (a) Motoring and (b) regenerative braking modes.

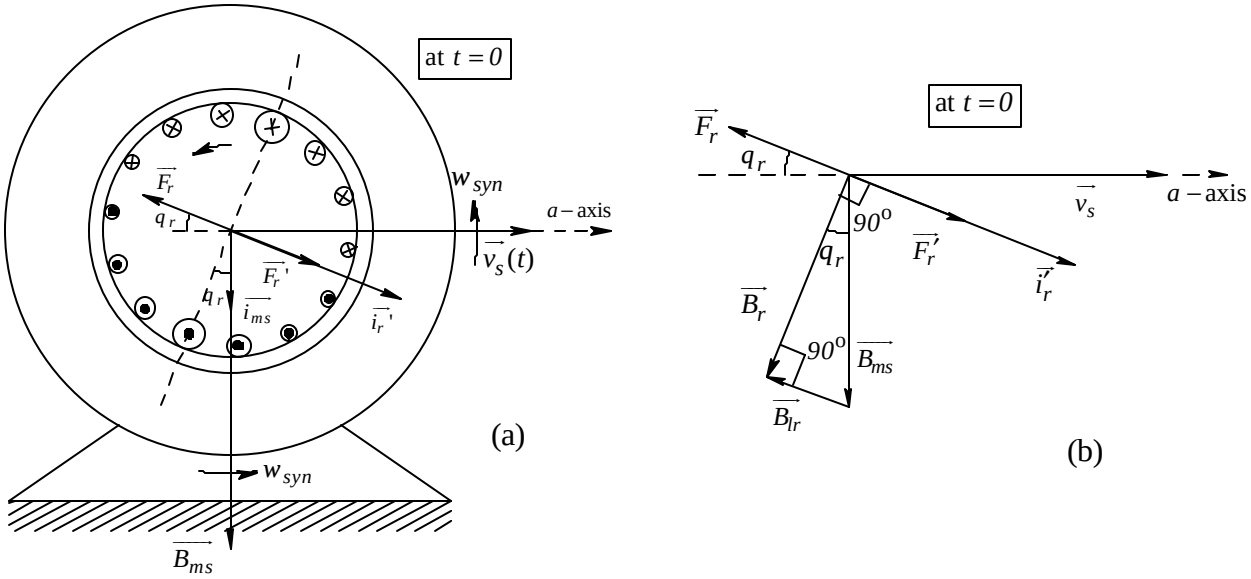

Fig. 20 Including the Rotor Leakage Flux.

Including The Rotor Leakage Inductance. In the presence of the rotor leakage flux, the maximum currents exist in the bars, which were "cut" by the peak flux density some time earlier (Fig. 20a). The space vector analysis shows the rotor-current produced mmf and the additional currents drawn by the stator winding, represented by $\vec{i}_r'$ (Fig. 20b). Another important observation is that the rotor flux density $\vec{B}_r$ $(= \vec{B}_{ms} + \vec{B}_{\ell r})$ is now at angle of 90^0 to $\vec{i}_r'$. This condition is used in vector control discussed in the advanced course [6], where keeping the amplitude $\hat{B}_r$ of the rotor flux-density constant, the torque component of the stator current is controlled to result in an almost instantaneous change in torque without oscillations (i. e., the machine instantly goes from one steady state to the next). The resulting phasor diagram and the per-phase equivalent circuit are shown in Fig. 21. The stator resistance and the leakage inductance are added to the per-phase equivalent circuit to complete the discussion.

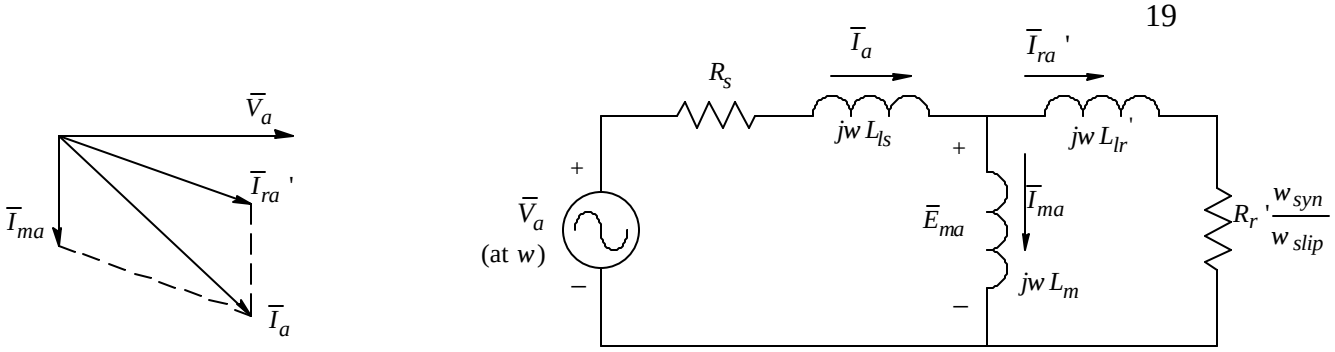

Fig. 21 Phasor diagram and the per-phase Equivalent circuit.

Control of Electric Drives. To give students a system's perspective, it is useful to discuss or at least present a one-lecture overview (depending on the time available) of how such drives are controlled [7]. Using a brush-type dc motor, the design of P-I regulators in a cascade control (Fig. 22) can be quickly described. We can point out that the same procedure is used in the advanced drives course for designing the controllers in the flux and the torque loops of vector-controlled ac drives.

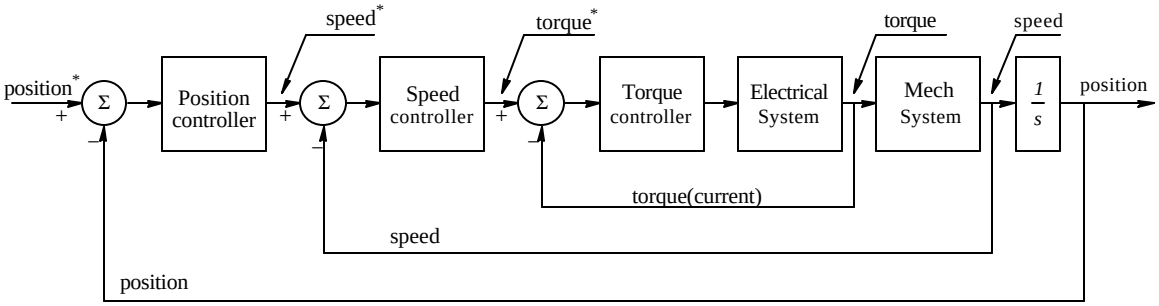

Fig. 22 Cascade control of a motor drive.

Power-Quality Issues. Electric drives can contribute to degradation of the utility power supply quality. At the same time, electric drives are susceptible to power system disturbances. An overview of these interactions can be presented in one to two lectures, leaving the details to be discussed in the power electronics courses.

Role of Simulations in the First Course. The first course deals primarily with steady state analysis. Therefore, the role of computer simulations is useful in the discussion of power electronics and controls related topic. For this purpose, programs such as PSpice™ or SIMULINK™ can be used. In the advanced course, use of simulation plays an essential

role, and we at the University of Minnesota have opted to use SIMULINK™. This choice is based on its capability, ease of its usage and widespread availability. Moreover, it is needed for the hardware laboratory being developed, described in the next section.

Real-Time, DSP-Based Electric Drives Hardware Lab [3]. Being developed by NSF and NASA funding in consultation with the consortium of nine universities and four government labs, this laboratory is intended to serve as the model for adoption at other universities. Therefore, safety, transportability, ease of usage and low cost are very important factors. This laboratory is intended for use in the first course, but its flexible nature will allow it to be used in advanced courses as well as in graduate level research.

The block diagram of this software-reconfigurable lab setup is shown in Fig. 23. The dc-bus is opted to be at 42 V for safety reasons, mindful of large automotive applications as the auto industry switches from 12/14-V system to 36/42-V system in the coming years. It consists of a dc machine as an active load, controllable in all four quadrants. The common dc bus for both the converters results in only the system losses to be supplied by a small dc power supply.

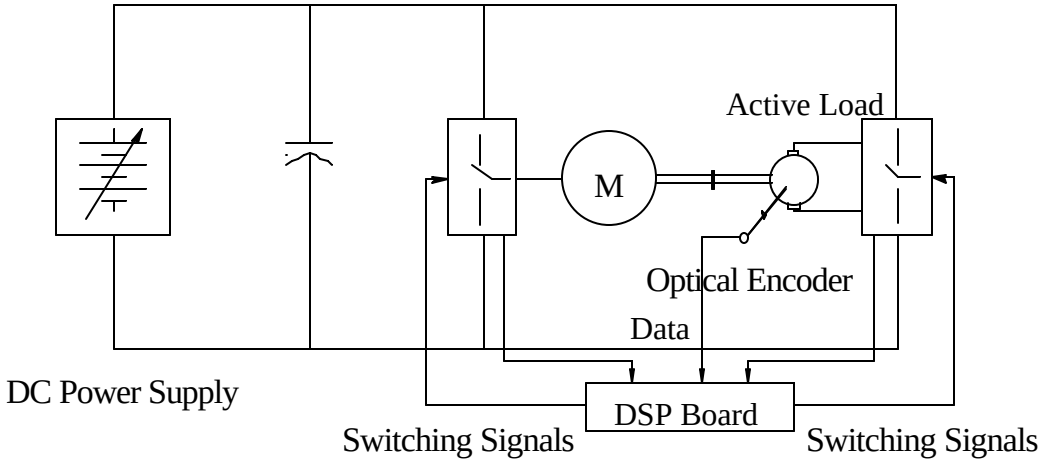

Fig. 23 DSP-based Lab.

This laboratory has three components: special motors are being built under a contract to operate from the converter fed by the 42-V dc bus. The converters are being developed

on a single board and the controller using pulse-width-modulation for speed and position control is based on a rapid prototyping tool from DSPACE [8]. In this system, students design the controller in SIMULINK by bringing various blocks together, and then a program (completely transparent to the users) converts the code and downloads it in an embedded micro-controller for real-time control of electric drives. It will offer an unparallel experience and will be a great means of attracting students and exciting their interest, where they will compare results of computer simulations with those of hardware experiments, providing them with an education that will be invaluable. An NSF-sponsored faculty workshop to describe this development and solicit comments is planned for September 2001 - March 2002 timeframe.

Conclusions

This tested approach is designed to breath new life into machines-related courses, thus reversing the trend of declining enrollments in this field with tremendous opportunities. The most important aspect of this effort is the first course on this subject, where we teach electric drives without the prerequisite of electric machine theory. A possible sequence of topics totaling ~40 lectures (50 minutes each) is presented below. We sincerely welcome your comments.

Topic	Number of Lectures
Introduction to Electric Drive Systems	1
Understanding Mechanical System Requirements	2
Review of Electric Circuits	1
Basic Understanding of Switch-Mode Power Electronics	4
Magnetic Circuits	5
Basic Principles of Electro-Mechanical Energy Conversion	3
DC-Motor and ECM Drives	5
Introduction to AC Machines and Space Vectors	5
Brushless DC (PMAC) Drives	4
Induction Machines: Steady State Analysis	5
Adjustable-Speed Induction-Motor Drives	3

Optional Topics

Feedback Controller Design
Power Quality Issues
Reluctance Drives

References:

1. NSF-Sponsored Faculty Workshops on *Teaching of Electric Drives and Power Electronics*, held at the University of Minnesota, 1994, 1997 and 1998.
2. N. Mohan, *Electric Drives: An Integrative Approach*, a textbook published by MNPERE, Minneapolis, 2001.
3. NSF/NASA-Sponsored Project, "DSP-based, Software-Reconfigurable Laboratory to Nationally Revitalize Electric Drives and Power Electronics Curricula, University of Minnesota, June 1, 2000 – May 31, 2003.
4. Turning Point Newsletter, Department of Energy, November 1998.
5. N. Mohan and J. Ramsey, Comparative Study of Adjustable Speed Drives for Heat Pumps, EPRI Final Report EM-4704, Project 2033-4, August 1986.
6. N. Mohan, Advanced Electric Drives: Analysis, Control and Modeling using SIMULINK™, to be printed in August 2001 by MNPERE, Minneapolis, MN.
7. Instructor's CD to accompany [2].
8. DSPACE GmbH, Technologiepark 25, 33100 Paderborn, Germany.